Suitability of the Coralline Alga *Clathromorphum compactum* as an Arctic Archive for Past Sea ice Cover

Natasha Leclerc[1], Jochen Halfar[2], Steffen Hetzinger[3], Phoebe P.T.W. Chan[4], Walter Adey[5], Alexandra Tsay[6], Eric Brossier[7], and Andreas Kronz[8]

[1] Earth Sciences Department, University of Toronto, 22 Russell Street, Ontario M5S 3B1, Canada

[2] Chemical and Physical Sciences Department, University of Toronto Mississauga, 3359 Mississauga Road N., Ontario L5L 11C6, Canada

[3] GEOMAR Helmholtz-Zentrum für Ozeanforschung Kiel, Wischhofstr. 1-3, 24148 Kiel, Germany

[4] Department of Earth Science, University of Bergen and Bjerknes Centre for Climate Research, Jahnebakken 5, Bergen 5007, Norway

[5] Botany Department, Smithsonian National Museum of Natural History, 1000 Constitution Avenue, NW, Washington D.C. 20560, USA

[6] Department of Earth Sciences, University of Geneva, Rue des Maraichers 13, 1205, Geneva, Switzerland

[7] Association Nord-Est, Lanton, Hanvec, France

[8] Geowissenschaftliches Zentrum, Universität Göttingen, D-37077 Göttingen, Germany

Corresponding author: Natasha Leclerc (natasha.leclerc@mail.utoronto.ca)

Key Points:

- Annual proxy anomalies from growth increments and Mg/Ca ratios in calcareous algae were compared to satellite sea ice concentrations
- Algal growth anomalies most significantly correlated to sea ice concentrations at sites with medium wave exposure and >5 months sea cover
- Downsampled to five-year averages, correlations are strengthened and can capture summer sea ice concentrations better than annual averages

Abstract

Arctic sea ice cover has been steeply declining since the onset of satellite observations in the late 1970s. However, the available annually resolved sea ice data prior to this time are limited. Here, we evaluated the suitability of annual trace element (Mg/Ca) ratios and growth increments from the long-lived annual increment-forming benthic coralline red alga, *Clathromorphum compactum,* as high-resolution sea ice cover c. It has previously been shown that growth and Mg/Ca of *C. compactum* are strongly light controlled and therefore greatly limited during polar night and underneath sea ice cover. We compare algal data from 11 sites collected throughout the Canadian Arctic, Greenland and Svalbard, with satellite sea ice data. Our results suggested that algal growth anomalies most often produced better correlations to sea ice concentration than Mg/Ca alone or when averaging growth and Mg/Ca anomalies. High Arctic regions with persistently higher sea ice concentrations and shorter ice-free seasons showed strongest correlations between algal growth anomalies and satellite sea ice concentration over the study period (1979-2015). At sites where ice breakup took place prior to the return of sufficient solar irradiance, algal growth was most strongly tied to a combination of solar irradiance and other factors such as temperature, suspended sediments, phytoplankton blooms and cloud cover. These data are the only annually resolved in situ marine proxy data known to date and are of utmost important to gain a better understanding of the sea ice system and to project future sea ice conditions.

Plain Language Summary

Natural layered structures such as tree rings and mollusk shells' growth layers archive environmental data in their rings or layers as they grow. A lesser known and emerging environmental archive is the coralline red algae species, *Clathromorphum compactum*, that lives on the Arctic and North Atlantic seafloor (10-30m deep). It grows on solid substrate by forming a new calcified layer of growth every year, ultimately building up dome-like crusts over tens or hundreds of years. Different thicknesses and amounts of magnesium in their annual layers depend on ocean temperature and sunlight availability. Because sea ice forms under cold conditions and blocks sunlight from reaching the sea floor, we hypothesized that magnesium chemistry and growth also responded to sea ice conditions. Here, we evaluated the relationship

between algal layer thicknesses and/or magnesium chemistry to sea ice data derived from satellite images at 11 sites. Strong relationships between algal growth and sea ice cover were found at exposed sites with longer seasonal-ice cover duration. Recent reduction of sea ice in certain regions have weakened the growth-sea ice relationship. A deeper understanding of past ice conditions can provide extremely valuable data for climate models to more accurately predict future sea ice scenarios.

1 Introduction

1.1 Sea ice effects on global climate change and lack of long-term high-resolution sea ice records

Summer sea ice extent has declined by 12.9 % per decade since 1979 relative to the 1981-2010 average (Cavalieri & Parkinson, 2012; Comiso, Meier, & Gersten, 2017). This alarming rate of decline has potentially devastating impacts on Arctic ecosystems, and destabilizing effects on ocean circulation, global climate, and human populations due to the connection of sea ice to multiple feedback mechanisms including the ice-albedo feedback (Meier et al., 2014). However, current climate model projections are unable to fully capture annual sea ice variability and often underestimate the amount of sea ice decline due to a limited understanding of the internal and anthropogenic processes driving sea ice loss (Ding et al., 2017). Models that project future climate scenarios utilize multiple past sea ice datasets and sea ice-related variables. The sea ice records with the highest temporal and geographical resolutions are derived from satellite datasets providing almost daily global coverage back to 1979. Sea ice records that extend further back than 1979 are made from aggregated datasets with lower geographic coverages and temporal resolutions. Sources include: stations, fishing, shipping, navy, research vessels, experiments, exploration expeditions, buoys, historical data sources (Polyak et al., 2010; Worley, et al., 2005). However, these datasets are spatially and temporally discontinuous. For instance, historical observations were biased toward the ice margins due to the constraints of penetrating the ice pack. In addition, whale and seal hunting data sources excluded internal ice pack regions since marine life is typically more abundant along ice margins (e.g., Hill & Jones, 1990; Mahoney et al., 2011; Walsh et al., 2017).

1.2 Paleo-sea ice proxies: strengths and limitations

Proxy information can yield sea ice information from less accessible internal sea ice regions and further back in time. Terrestrial sea ice proxies such as ice cores from ice sheets, tree-ring records, and lake sediments can provide information on thermal conditions affecting sea ice formation and melt (e.g., Kinnard et al., 2011) but are remote from sea ice regions and may only yield limited information on the dynamics of sea ice. Meanwhile, marine proxies from sediment cores provide better information on sea ice dynamics that can extend back millennia. The highly branched isoprenoid biomarker with 25 carbon atoms (IP25) found in ocean sediments can establish the presence or absence of seasonal sea ice as it is originally formed in first-year ice and brine channels (Belt et al., 2007), while the quantitative open-water phytoplankton-IP25 index (PIP25) can further quantify the concentration of sea ice cover and changes in distribution (Belt, 2019; Köseoğlu, et al., 2018; Müller et al., 2011; Stein & Fahl, 2013). However, regional sedimentation rates are a limiting factor for proxies based on ocean sediment cores, yielding sub-decadal resolution data only in the best situations with interpolated two- to five-year resolutions (Backman, et al., 2004; Belt et al., 2012; Ran, et al., , 2011; Sicre, Jacob, et al., 2008; Sicre, Yiou, et al., 2008). Further, the use of assemblage analyses based on the identification and quantification of diatoms, foraminifera, ostracods and dinoflagellate cysts (i.e., dinocysts) can also be challenging due to their presence in both perennial and seasonal sea ice cover environments (Gemery et al., 2017; Kucera et al., 2005; Seidenkrantz, 2013). Since all sea ice proxies are geographically and temporally limited, a network of proxy records is needed to capture the full extent of spatial and temporal variability of sea ice dynamics and thermodynamics in the Arctic (Kaufman, 2009). Accordingly, high-resolution proxies that provide annual or seasonal sea ice information for the past millennia are necessary to calibrate climate models that project future sea ice behavior.

1.3 The coralline red alga sea ice proxy

An emerging archive for Arctic sea ice conditions is the coralline red algae species *Clathromorphum compactum* (Halfar et al., 2013; Hetzinger, et al., 2019), a calcifying alga that grows ubiquitously in near-shore arctic and subarctic environments including the North Atlantic and the Bering Sea where rock and boulders cover the shallow benthic seafloor (Adey, 1965;

Adey, Halfar, & Williams, 2013). *C. compactum* produce tree-ring-like annual growth increments in their calcified ($CaCO_3$) skeletons that are high in magnesium (Adey et al., 2013) (Figure 1). These slow growing and long-lived algae can grow upwards of 600 years (Halfar et al., 2013). As they grow, they deposit layers of calcified cells in varying sizes and cell wall thicknesses that result in increments of lighter and darker bands (Foster, 2001). Experimental tank studies of *Clathromorphum* sp. have shown that their growth is highly dependent on both sunlight and temperature (Adey, 1970; Williams et al., 2018). Additionally, the variability of magnesium to calcium ratios (Mg/Ca) found in *C. compactum*'s annual growth layers is cyclical and strongly correlates with seasonal changes in surrounding sunlight availability and temperature (Williams et al., 2018). *C. compactum* produces its normal range of tissues with similarly complex high-magnesium calcitic wall structures both in the light and in the dark. However, growth is dependent upon the production and storage of photosynthate. Growth and calcification can occur for at least two months in the dark, at which point it ceases, following the exhaustion of stored photosynthate (Williams et al., 2018). The crust can exist for long periods without light, growth or photosynthesis, and growth will resume with the return of new light for photosynthesis. Furthermore, growth rates have been shown to vary according to latitude and regional sunlight access (Halfar et al., 2013). Accordingly, growth rates are higher in coastal Maine (43°N) (400 μm/yr), as compared to southern Labrador (52°N) (240 μm/yr), and the Canadian Arctic Archipelago (73°N) (61 μm/yr) (Halfar et al., 2013). As growth and Mg/Ca ratios of *C. compactum* have been shown to be stimulated through photosynthesis, blocking of sunlight by seasonal sea ice cover has been hypothesized to reduce the widths of annual growth increments and reduce annual Mg/Ca ratios.

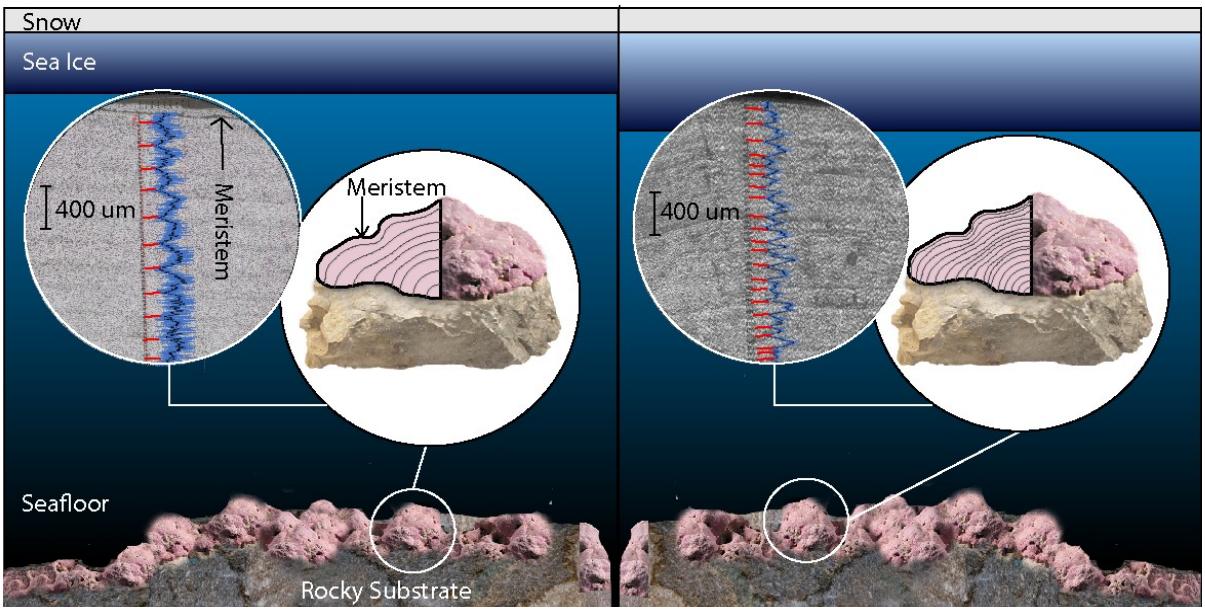

Figure 1. Schematic representation of relationship between length of sea ice cover and *C. compactum* growth and Mg/Ca ratios. Left panel indicates shorter duration of thin sea ice cover and thicker growth increments in depicted cross-section. Right panel indicates longer period of thick sea ice cover and consequently thinner algal growth increments. Mg/Ca ratios, superimposed on high-resolution image of internal growth increments, are cyclical on annual timescales and match annual growth rates. Annual Mg/Ca minima are indicated with red lines and line-up with darker slow growth (winter) $CaCO_3$ layers. The meristem, typically, lying 5-10 cells below the algal surface is where algal growth and calcification occur. The overlying epithallus, weakly calcified and often grazed by molluscs, is ephemeral and location of most photosynthesis. Calcified tissue underlying meristem, the perithallus, builds up annual increments that provide multiannual proxy data.

It has previously been shown that a combination of normalized growth rates and Mg/Ca ratios (i.e., algal anomalies) significantly inversely correlated with satellite-derived sea ice concentrations near algal collection sites in Arctic Bay (Nunavut) and the Kingitok Islands (Labrador) in Canada (Halfar et al., 2013). This suggested that when there was a longer duration of higher sea ice concentrations, less light reached the seafloor during the year, producing less growth (thinner increments) and reduced Mg incorporation (lower Mg/Ca ratios). Furthermore, a recent proxy time series of *C. compactum* from Svalbard, Norway, showed significant

correlations between algal anomalies and regional sea ice concentration data and other Arctic sea ice proxy reconstructions, which demonstrated a reduction of sea ice and a general warming trend in Svalbard over the 20st century (Hetzinger et al., 2019).

In order to assess the robustness of sea ice proxies, fundamental questions regarding their strengths and weaknesses and the geographic and temporal contexts in which each proxy can be applied must be answered (De Vernal, et al., 2013). While, the above-mentioned studies have established the potential for *C. compactum* to be used for sea ice reconstruction, the strengths and weaknesses of the algal anomaly sea ice proxy have not been assessed in a multi-site comparison across the Arctic landscape. Furthermore, while the combination of Mg/Ca ratios and growth increment data has been correlated to sea ice concentration, it has not been established if both equally show a relationship or if one anomaly alone could be used exclusively to compare to sea ice conditions. In this study, we investigate 30 *C. compactum* samples across 11 sites encompassing Svalbard (Norway), Western Greenland, Eastern Labrador (Canada), and multiple locations in Nunavut (Canada) (Figure 2). Their individual relationships to regional sea ice conditions were evaluated by determining the degree of correlation to satellite-derived sea ice concentration datasets, ice charts and satellite images.

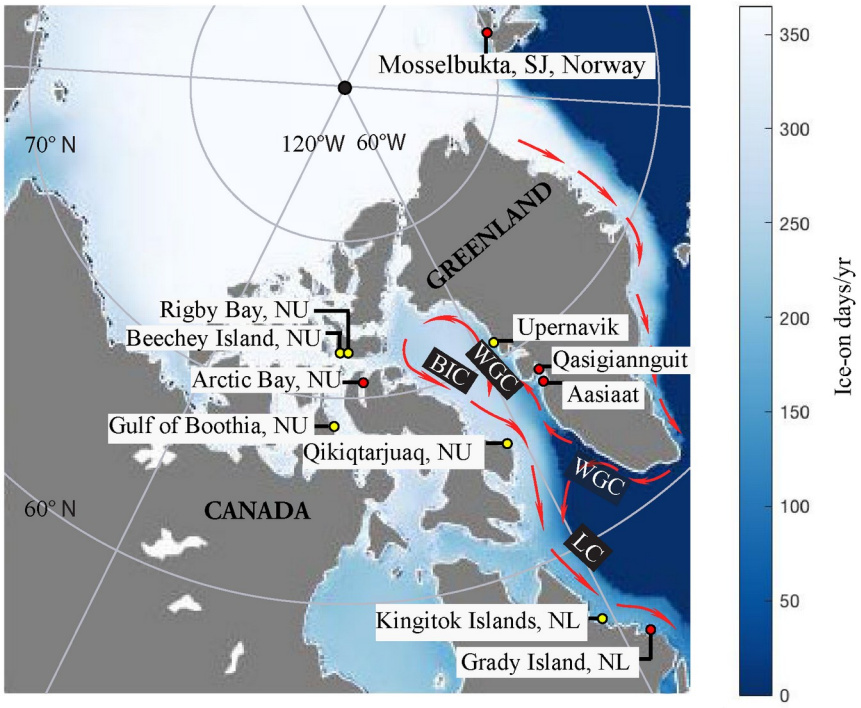

Figure 2. Studied arctic and subarctic *C. compactum* collection sites in Nunavut (NU) and Labrador (NL) in Canada, Greenland, and Svalbard (SJ) in Norway. Yellow dots indicate sites with significant relationships between summer sea ice concentration (SIC_{SUMMER}) and algal growth while red dots indicate sites with insignificant relationships that also tend to have shorter durations of ice cover near the ice margin. Average number of ice-on days with >15% ice cover over study period (1979-2015) shown graded from white (365 days) to dark blue (0 days). Currents depicted in black boxes: West Greenlandic Current (WGC); Labrador Current (LC) and; Baffin Island Current (BIC). Data source: daily NSIDC sea ice concentration dataset 25-km resolution.

2 Materials and Methods

2.1 Sample collection and preparation

Live specimens of *Clathromorphum compactum* were collected in 2008, 2010, 2011, 2014, and 2016, via SCUBA from 10-20 m depth (Figure 2, Table 1). Samples were cut along the axis of growth to expose growth layers with an Isomet precision saw. Samples were then polished with 9 µm, 3 µm, and 1 µm diamond-polishing suspension solutions on a Struers Labopol polishing disk and placed in an ultrasonic bath between polishing steps to remove adhering media. Sample cross-sections were imaged with an Olympus VS-BX reflected light microscope and automated stage using Geo.TS software (Olympus Soft Imaging Systems) that generated photomosaics of imaged area. From these images, the samples providing the longest records, regular growth, and presenting the least disruptions (e.g., cracks, disrupted growth, or conceptacles – reproductive structures of the alga) were selected for geochemical analysis. Samples were also inspected to ensure a visible meristem and epithallus – the growing edge and protective layer of the organism exposed to light – to confirm the deposition date of the first calcified perithallial layer beneath (i.e. at time of collection) (Figure 1).

2.2 Analytical protocols for Mg/Ca and growth increment measurements

Specimens from Svalbard, Greenland, Rigby Bay, Beechey Island and the Gulf of Boothia collected in 2016 had laser ablation paths digitized on Geo.TS and path coordinates transferred

to a NWR 193 UC laser ablation inductively coupled plasma mass spectrometer (LA-ICP-MS) system coupled with an Agilent 7900 quadrupole mass spectrometer at the University of Toronto's Earth Science Centre. Measurements of Mg/Ca were obtained by conducting continuous laser ablation line scans at 5 μm/sec speed, an aperture size of 10 x 70 μm and 10 Hz pulse rate. Samples from Arctic Bay, Kingitok Islands and Qikiqtarjuaq, collected in 2008, 2011, and 2014 respectively, were analysed for Mg/Ca using a JEOL JXA 8900 RL electron microprobe at the University of Göttingen with acceleration voltage of 10kV, beam current of 12nA and spot diameter of 3.5 μm with a spacing of 10 μm between measurements along the axis of growth (for details of method see Halfar et al., 2013). Samples collected from Grady Island in 2010 were analysed at the University of Mainz, Germany in the Earth System Science Research Centre using an Agilent 7500 quadrupole-ICP−MS attached to a New Wave Research UP−213 laser ablation system. Ablation measurements were obtained with a 65 μm spot size along continuous transects, a 10μm/sec speed, 10 Hz pulse rate, laser energy density of 6 J/cm2, and helium carrier gas. All elemental data were calibrated with NIST SRM 610 standard (see details in Hetzinger et al., 2011). Resulting Mg/Ca data for all analyzed specimens was down-sampled to 12 measurements/year resolution with AnalySeries software (Paillard et al., 1996). When two measurement transects were taken from a sample, annual growth increment widths and Mg/Ca ratios were averaged between transects and were compared to aid in the construction of age models. Growth increment widths were calculated by measuring the distance between the time-stamped laser ablation measurements or electron microprobe spot measurements of two sequential Mg/Ca minima representing the space of one year (red lines, Figure 1). Both growth increment and Mg/Ca measurements were normalized into unitless anomalies. Annual growth increment and Mg/Ca anomalies were evaluated separately and also averaged to produce combined algal proxy anomalies.

2.3 Satellite datasets and spatial correlations

Combined algal anomalies were regressed against monthly and annually averaged sea ice concentrations (SIC) from the gridded National Snow & Ice Data Centre (NSIDC) Sea ice Concentration Dataset (Version 3) that extend from 1979 to present (https://nsidc.org/data/g02202; Peng et al., 2013). These data were obtained through passive

241 microwave sensors Nimbus-7 SMMR and DMSP SSM/I-SSMIS that measure surface brightness
242 converted to 25 x 25 km gridded sea ice concentrations via algorithms that also reduce the bias
243 between different instruments used during the satellite era (Meier et al., 2017; Peng, et al., 2013).
244 Due to some sites being incorporated in gridded cells classified as land, SICs from the cells
245 surrounding all collection sites were averaged when calculating correlations between regional
246 sea ice conditions (75-km resolution) and algal anomalies. Data gaps were found in December
247 1987 to January 1988 and were therefore not used in the calculation of annual SIC averages.
248 Daily NSIDC SIC 25-km resolution dataset was used to determine the average number of ice-
249 free days (<15%) per year for the 75-km gridded area around each of the collection sites. SIC
250 monthly means that significantly inversely correlated with algal anomalies ($p < 0.05$) were
251 pooled together by averaging these months' SIC, which were then statistically regressed against
252 algal anomalies. Regional maps displaying spatial regression analyses of algal anomalies and sea
253 ice concentrations were generated with MATLAB version R2018a and m_map add-on. Sea
254 surface temperatures from HadISST dataset at a 1° resolution (Rayner et al., 2003) were also
255 used to conduct regression statistics between algal anomalies and nearest 1° grid cell values
256 (https://www.metoffice.gov.uk/hadobs/hadisst/). The Norwegian Meteorological Institute's
257 archived nearly daily sea ice charts (1997-2015) for the Fram Strait and Svalbard regions (https://
258 cryo.met.no/archive/ice-service/icecharts/quicklooks/) and satellite imagery from NASA
259 Worldview (https://worldview.earthdata.nasa.gov) were used to examine sea ice concentrations
260 at a higher spatial resolution than the NSIDC dataset. Satellite cloud fraction cover data
261 (EUMETSAT/CMSAF; 0.25° resolution) obtained from KNMI Climate Explorer
262 (climexp.knmi.nl/select.cgi?cfc_cmsaf;
263 http://dx.doi.org/10.5676/EUM_SAF_CM/CLARA_AVHRR/V002), and monthly chlorophyll α
264 concentrations (MOSISA_L3mCHL v2018; 4-km resolution) were obtained through NASA
265 Earth Data's tool Giovanni (https://giovanni.gsfc.nasa.gov;
266 data/10.5067/AQUA/MODIS/L3M/CHL/2018). Linear regression tests were run between algal
267 anomalies and monthly or annual SIC averages and durations of ice-free season for all sites (75-
268 km resolution). Multiple months' SICs were averaged when algal anomalies correlated with
269 more than one monthly SIC (SIC_M), which were restricted to the highest solar irradiance season
270 of May to October (Adey et al., 2013). SIC_M means were then regressed against algal anomalies.
271

272 **Table 1.** *Sample information for this study and time period compared to satellite records*
273

Site	Latitude/ Longitude	Sample ID	Measurement transects/sample	Period analyzed
Svalbard, Norway				
Mosselbukta	79°55'37.0"N 15°54'07.9"E	Sv1	2	1979-2014↓
		Sv18	1	1979-2015
		Sv28	2	1979-2015
		Sv47	1	1979-2015
		Sv90	2	1979-2015
West Greenland				
Aasiaat	68°44'9.83"N 52°32'10.86"W	2016_1_19	2	1979-2015
		2016_1_46	2	1979-2015
Qasigiannguit	68°53'51.54"N 51°16'54.19"W	2016_4_2	2	1979-2015
		2016_4_29	2	1988-2015
Upernavik	72°23'2.94"N 55°31'50.77"W	2016_7_21	2	1979-2015
		2016_7_27	2	1979-2015
		2016_7_30	2	1979-2015
East Labrador, Canada				
Grady Island	53°47'60.00"N 56°24'30.00"W	10-18_18-20	2	1979-2008↓
		10-18_15-17	2	1978-2008↓
Kingitok Islands	55°23'53.88"N 59°50'48.12"W	Ki1	1	1979-2010
		Ki2	1	1979-2010
Nunavut, Canada				
Qikiqtarjuaq	67°2'17.52"N 62°14'56.76"W	2014_4_1	2	1979-2012↓
		2014_4_2	2	1980-2012↓
		2014_4_3	2	1979-2012↓
Gulf of Boothia	70°24'18.12"N 91°50'39.3"W	16_49_80	2	1979-2015
		16_49_131	2	1979-2015
Arctic Bay	73° 1'2.64"N 85° 9'12.96"W	AB1	1	1979-2007
		AB30	1	1979-2007
		AB31	2	1979-2007
Rigby Bay	74°33'37.50"N 90° 1'54.48"W	16_22_11	2	1979-2015
		16_22_39	2	1979-2015
		16_22_90	2	1979-2015
Beechey Island	74°42'54.46"N 91°47'29.35"W	16_24_2b	2	1979-2015
		16_24_15	2	1979-2015
		16_24_41b	2	1979-2015

274 Note. Downward arrows indicate that a one-year lag was identified in the time-series.

3 Results

3.1 Annual mean Mg/Ca and growth increment comparison

Based on our hypothesis, algal growth and Mg/Ca anomalies were expected to demonstrate a negative correlation to annual (SIC_A), monthly (SIC_M) or summer (SIC_{SUMMER}) SIC, and a positive correlation to the duration of the ice-free period. Mg/Ca ratios and growth increments were regressed independently against annual sea ice concentrations (SIC_A) to determine whether they equally contributed to correlations between SIC_A and the combined algal anomalies. The results revealed that both growth increments and combined algal anomalies had the strongest significant negative correlations with SIC_A at four sites (Figure 3). However, growth increment anomalies alone outperformed the other proxies by producing significant negative correlations with SIC_A at seven sites compared to five and four for combined algal anomalies and isolated Mg/Ca anomalies, respectively (Figure 3). Since the results suggest a more robust relationship between growth increments and SIC_A at most sites, the rest of the results and discussion will focus only on the growth increment anomaly results.

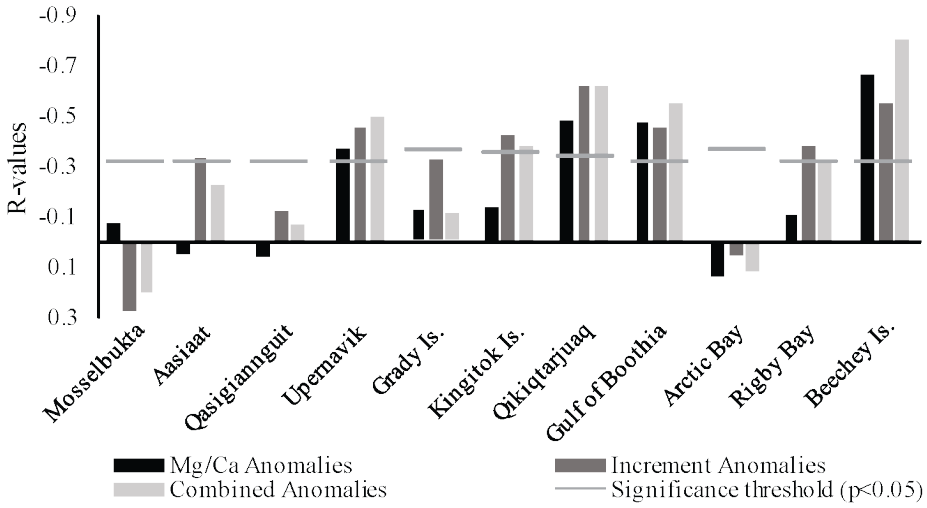

Figure 3. Mg/Ca, growth increment, and combined algal anomalies regressed against SIC_A (1979-sample collection date). Horizontal lines indicate threshold for significance ($p<0.05$).

3.2 Relationship between sea ice and algal growth anomalies

298 Regression results showed that algal growth anomalies at 7 out of 11 sites had significant
299 negative correlations with SIC_A ($p<0.05$), 2 of which tested as significantly positive correlations
300 with the annual durations of the ice-free period (i.e., days with <15% SIC; Table 2). Algal
301 anomalies from 8 sites significantly inversely correlated with at least one month of the monthly
302 resolved NSIDC dataset (SIC_M) during the study period (Table 2). Among these, Aasiaat showed
303 a negative correlation to May only, when sea ice typically breaks up in this location. While the
304 annual SIC averages were used for comparison (SIC_A), previous studies suggested that growth
305 resumes after a winter shutdown, once solar irradiance reaches the seafloor when sea ice breaks
306 up (Adey et al., 2013). Accordingly, summer month SIC averages (May-October) were isolated
307 from the annual dataset and compared to growth anomalies. Six sites had growth anomalies that
308 significantly correlated with SIC_{SUMMER}. Growth anomalies with non-significant correlations or
309 low significance to regional SIC tended to be from sites closer to the ice margin with longer ice-
310 free periods (red dots; Figure 2). In comparison to annual means, regression results of five-year
311 running means were more significant (i.e., lower p-values), especially in regions with shorter ice-
312 free periods, at the majority of sites (N5; Table 2). Algal growth anomaly time series from
313 individual sites further show the synchrony with SIC_{SUMMER} at most sites (Figure 4).

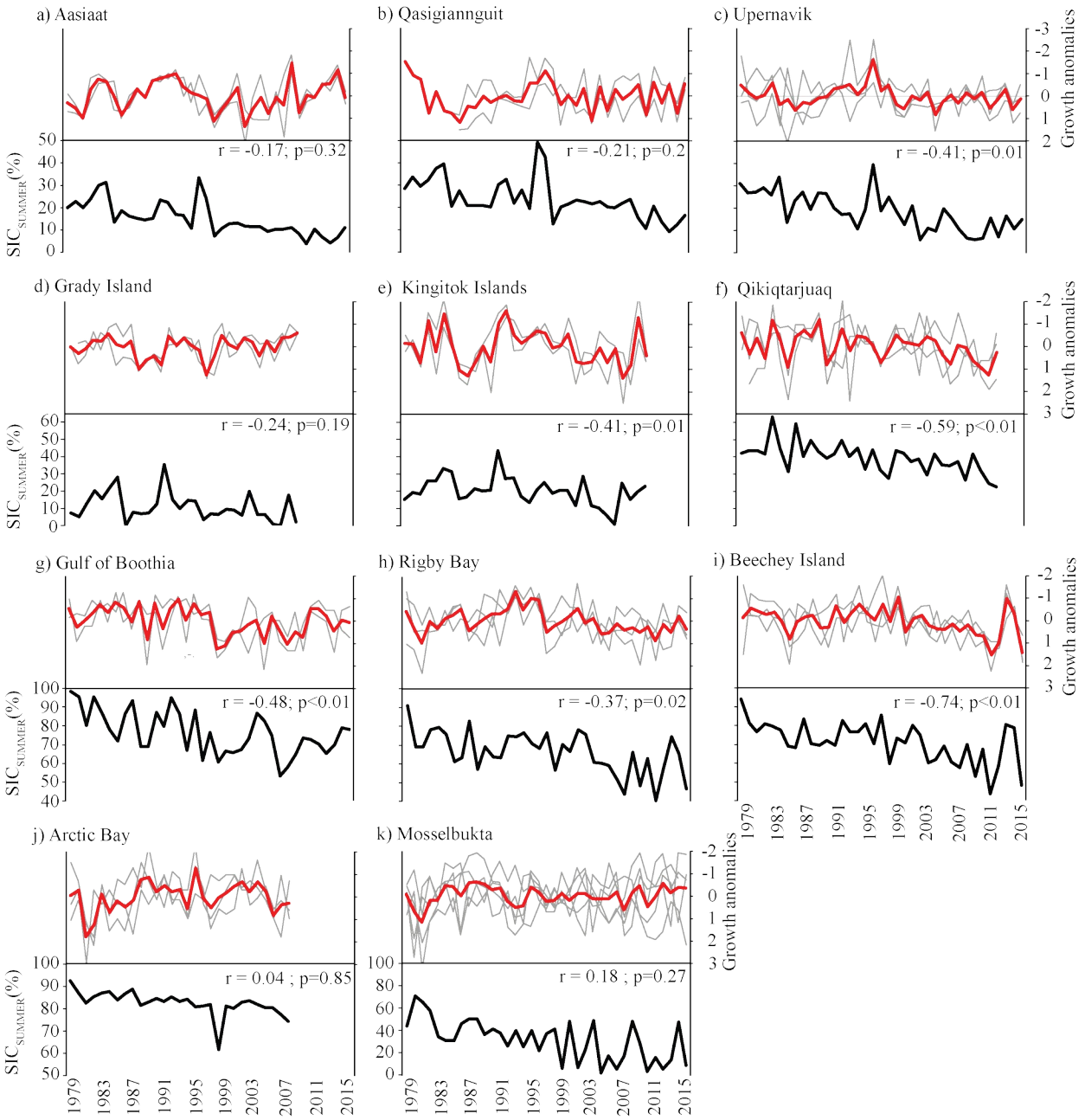

Figure 4. Algal growth anomalies (red) and SIC_{SUMMER} (black: May-Oct means) time series. Algal growth anomalies from individual samples in grey. Note that algal growth anomalies are presented on inverted axis.

Table 2

Results of regression analysis between growth increment anomalies and sea ice conditions (R- and p-values)

Site	Mean SIC_A	Mean Ice-free days	Correlations with growth increment anomalies															
			SIC_A (Jan-Dec)				SIC_M						SIC_{SUMMER} (May-Oct)				Ice-free days	
			R	p	$R_{(N5)}$	$p_{(N5)}$	Months (p<0.05)	R	p	$SIC_{M\ (N5)}$ (p<0.05)	$R_{(N5)}$	$p_{(N5)}$	R	p	$R_{(N5)}$	$p_{(N5)}$	R	p
Mosselbukta, NO	39%	217	0.27	0.1	0.01	0.95	**	**	**	**	**	**	0.18	0.27	-0.05	0.80	-0.004	0.98
Aasiaat, GL	36%	204	-0.34	0.04	-0.44	0.01	May	-0.40	0.02	May	-0.58	0.0004	-0.17	0.32	-0.23	0.19	0.14	0.41
Qasigiannguit, GL	45%	229	-0.13	0.46	0.03	0.86	Aug-Oct	-0.39	0.02	Aug-Oct	-0.68	0.00001	-0.21	0.20	0.06	0.76	0.001	0.99
Upernavik, GL	46%	218	-0.46	0.005	-0.49	0.004	Jun; Aug-Oct;	-0.45	0.005	May; Aug-Oct	-0.50	0.003	-0.41	0.01	-0.51	0.002	0.12	0.45
Grady Island, NL	38%	287	-0.30	0.10	-0.01	0.95	**	**	**	**	**	**	-0.24	0.19	-0.20	0.32	-0.11	0.56
Kingitok Islands, NL	44%	201	-0.42	0.015	-0.59	0.001	Jun-Jul	-0.44	0.01	May-Jul	-0.66	0.0001	-0.44	0.01	-0.66	0.0001	0.27	0.14
Qikiqtarjuaq, NU	67%	120	-0.54	0.001	-0.73	4.9E-06	Jul-Sep;	-0.66	2.1E-05	Jun-Aug; Oct	-0.81	4.4E-08	-0.59	0.0002	-0.78	3.5E-07	0.43	0.01
Gulf of Boothia, NU	88%	112	-0.46	0.004	-0.79	5.7E-08	Jun-Oct	-0.48	0.003	May-Oct	-0.78	5.4E-07	-0.48	0.003	-0.78	5.4E-07	0.33	0.04
Arctic Bay, NU	90%	190	0.06	0.77	0.47	0.02	**	**	**	**	**	**	0.04	0.85	0.37	0.07	-0.01	0.95
Rigby Bay, NU	82%	132	-0.38	0.02	-0.65	0.00004	Aug-Oct	-0.39	0.02	May-Jun; Aug-Oct	-0.70	4.7E-06	-0.37	0.02	-0.65	3.8E-05	-0.31	0.07
Beechey Island, NU	85%	130	-0.55	0.0004	-0.59	0.0003	May-Oct	-0.74	1.6E-07	May-Oct	-0.90	6.9E-13	-0.74	1.6E-07	-0.90	6.9E-13	-0.31	0.07

Note. Months falling between May and October that individually produced significant and negative correlations to algal growth anomalies are labelled under SIC_M: Months (p<0.05). Monthly SIC that significantly inversely correlated to algal growth anomalies when downsampled to five-year running means are labelled under $SIC_{M\ (N5)}$ (p<0.05). All mean values calculated for 1979 to year of collection. Significant correlations (p<0.05) shaded orange. Five-year running mean comparison indicated by N5 subscript. Sites with no significant correlating months indicated with two asterisks (**). Positive correlation to SIC and negative correlations to mean ice-free days shaded in grey.

330 3.3 Spatial patterns of sea ice correlation
331
332 Figure 5 illustrates that most sites had inverse relationships with regional SIC_{SUMMER}. Algal
333 growth anomalies from sites with the most significant negative correlations with SIC_{SUMMER}
334 tended to exhibit a strong regional relationship with large Arctic areas. For example, Beechey
335 Island had the strongest negative correlations around the collection site, but also had strong
336 correlations with most of the Canadian Arctic Archipelago, likely owing to similar regional sea
337 ice dynamics (Melling, 2002). On the Labrador coast, regional correlations around Kingitok
338 Islands and Grady Island were influenced by the Labrador Current with negative correlations
339 extending to the west coast of Greenland. The Baffin Island current seemed to be mostly
340 affecting the algal-sea ice relationship at Qikiqtarjuaq, while the West Greenlandic current
341 seemed to have most of an effect on Upernavik algal anomalies.

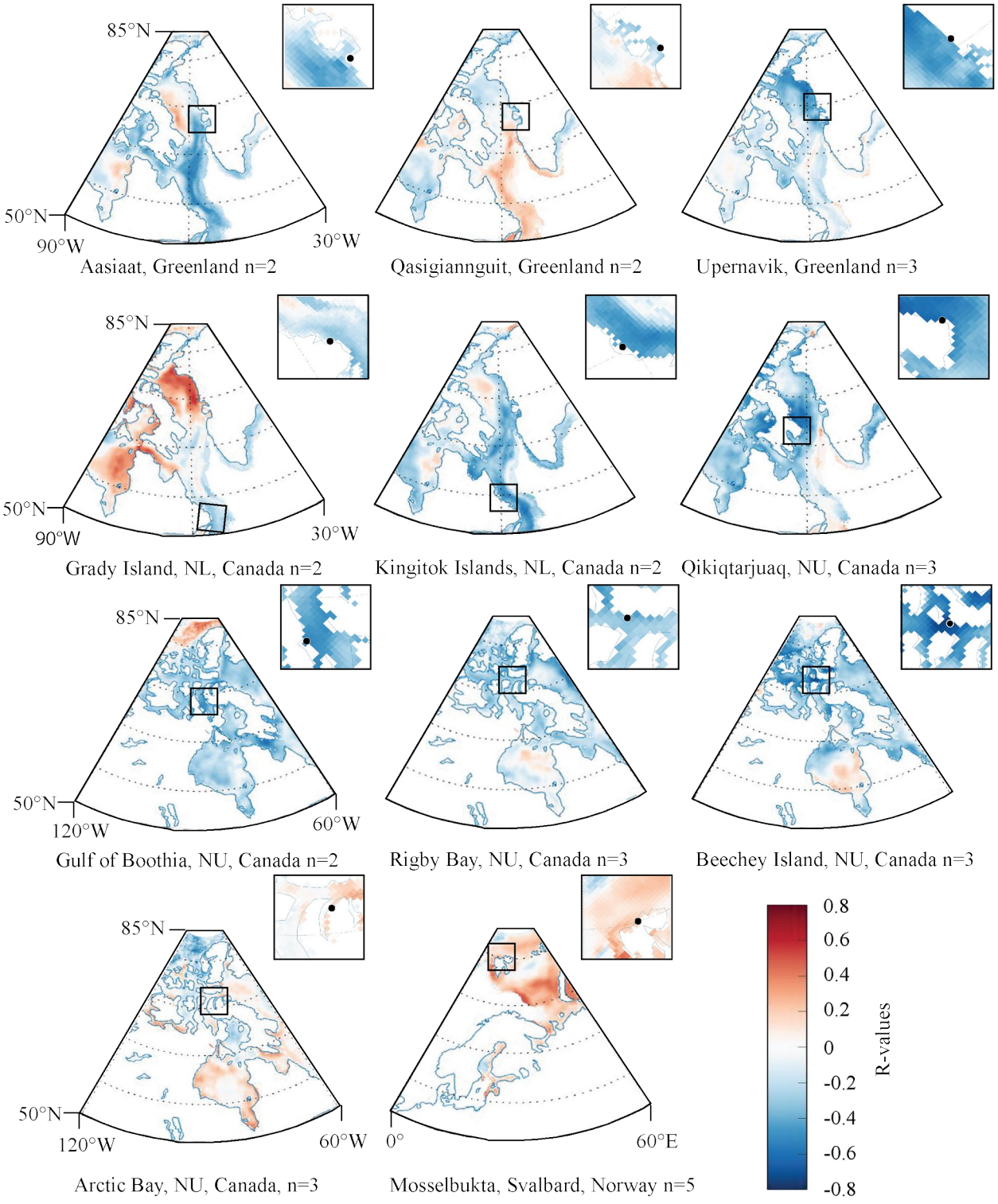

Figure 5. Spatial correlations between SIC_{SUMMER} and algal growth anomalies. SIC data retrieved from NSIDC Sea ice Concentration Version 3, monthly datasets. Spatial correlations calculated with Matlab mapping toolbox. Black dots in inset images indicate collection sites. Time series length varied depending on algal collection date: see Table 1.

347 3.4 Algal growth-temperature relationship

348

349 According to experimental results, *C. compactum* was expected to exhibit higher growth in
350 warmer SST conditions, therefore algal growth anomalies should positively correlate to SST to
351 demonstrate the growth temperature dependence (Williams et al., 2018). Correlations of algal
352 growth anomalies with SST_A and SIC_A were not significantly different (paired two-tailed t-test:
353 df=10, t=-2.09, p=0.06, CV=2.23) owing to the thermal relationship between sea ice and SST at
354 an annual resolution. SST_{SUMMER} correlated to algal growth anomalies at four sites, nearly half of
355 the sites that SIC_{SUMMER} significantly correlated to. SST_{SUMMER} also produced weaker relationships
356 to algal growth than did SIC_{SUMMER} (paired two-tailed t-test: df=10, t=-2.64, p=0.02, CV=2.23)
357 (Table 2 and 3). This indicated algal growth anomalies' strong seasonal sunlight dependence
358 reflecting *C. compactum*'s primary growing season in the summer.

359

360 **Table 3**

361 *Results of regression analysis between algal anomalies and SST (R- and p-values)*

362

Site	Mean SST_A (°C)	Correlations with growth anomalies						
		SST_A (Jan-Dec)		SST_M			SST_{SUMMER} (May-Oct)	
		R	p	Months (p<0.05)	R	p	R	p
Mosselbukta, NO	1.07	-0.24	0.15	Sep	0.44	0.006	-0.14	0.40
Aasiaat, GL	1.41	0.29	0.08	May	0.52	0.001	0.17	0.30
Qasigiannguit, GL	1.41	-0.07	0.70	**	**	**	0.05	0.75
Upernavik, GL	0.81	0.47	0.004	Aug-Sep	0.42	0.02	0.39	0.009
Grady Island, NL	2.49	0.27	0.14	**	**	**	0.08	0.68
Kingitok Islands, NL	1.14	0.31	0.08	Jul-Sep	0.51	0.003	0.44	0.01
Qikiqtarjuaq, NU	-0.63	0.47	0.005	Jul-Oct	0.53	0.0002	0.50	0.002
Gulf of Boothia, NU	-1.36	0.28	0.1	Jul	0.39	0.02	0.27	0.1
Arctic Bay, NU	-0.94	0.03	0.88	**	**	**	0.03	0.88
Rigby Bay, NU	-0.86	0.16	0.36	Sep	0.39	0.02	0.15	0.38
Beechey Island, NU	-1.01	0.57	0.0002	May-Oct	0.56	0.0003	0.56	0.0003

363 Note. Monthly SST falling between May and October that individually produced significant and
364 positive correlations to algal growth anomalies are labelled under SST_M: 'Months (p<0.05)'.
365 Significant correlations (p<0.05) shaded orange. Sites with no significant correlating months
366 indicated with two asterisks (**). Negative correlations shaded grey.

367

368 3.4 Temporal variability of algal - sea ice - temperature relationships

369

370 Temporal shifts in correlation between algal anomalies and SIC and SST were investigated
371 through the generation of 10-year running correlations. The temporal shift in correlation over the
372 past few decades indicated two overarching trends: 1) reduction of proxy strength in recent
373 decades due to the rapid reduction of sea ice; 2) increasing proxy strength in recent years due to
374 higher inter-annual sea ice variability (Figure 6). However, due to the short duration of records
375 and thus low sample size, many of the correlations are not significant (n=10/running correlation).

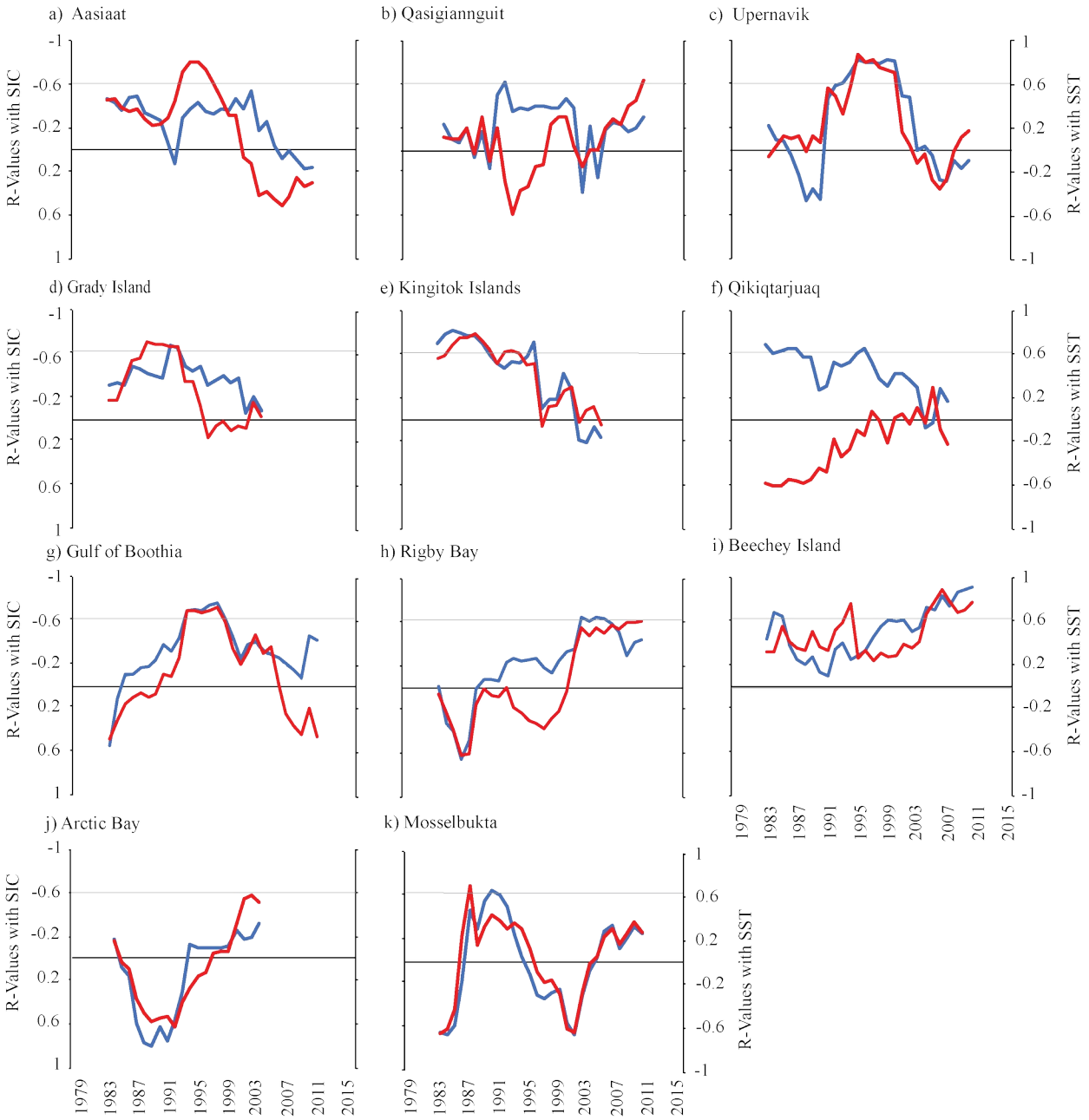

Figure 6. Results of 10-year running correlations with linear regression between algal growth anomalies and mean SST_{SUMMER} and SIC_{SUMMER} (May-Oct). Red line represents correlations with summer SST, and blue line represents correlation with summer SIC. Grey horizontal line indicates 95% significance threshold.

Algal anomalies in Aasiaat, Greenland, had strong correlations to SIC in the early record, followed by weaker correlations in the late record into the 2000s (Figure 6a). Notably, the late record is marked by increased inter-sample algal anomaly variability (Figure 4a). In addition,

385 when comparing the relationship between SIC_{SUMMER} and growth time series (Figure 4b) and how
386 it has changed through time at Qasigiannguit (Figure 6b), periods of low inter-annual SIC_{SUMMER}
387 variability (1999-2015) produced algal anomalies that did not strongly correlate to sea ice
388 records. Correlations with SIC_{SUMMER} were periodically stronger than SST_{SUMMER} in the earlier and
389 mid-section of the satellite record, yet not significant, however the relationship with temperature
390 has increased since the early 2000s (Figure 6b). Upernavik also had stronger algal-sea ice
391 relationships in the early record, that weakened in the 1990s when sea ice became completely
392 absent in July after 1996 (Figure 6c). Kingitok Islands and Grady Island (Figure 6d; 6e) results
393 showed that correlations with SIC and SST were stronger in the early record than in the late
394 record. Kingitok Islands and Grady Island experienced a significant reduction of sea ice after
395 1995. Accordingly, correlations with SIC_{SUMMER} and SST_{SUMMER} were stronger prior to 1995 and
396 correlations are generally weaker in recent years as temperatures have been relatively stable and
397 cloud cover has reduced. On the other hand, Qikiqtarjuaq, Gulf of Boothia, Rigby Bay and
398 Beechey Island experienced a steady decline in SIC since the beginning of the satellite record but
399 retained a higher concentration of sea ice for longer periods compared to other studied regions
400 (Figure 4). Algal growth anomalies generally track the lower and higher ice years but cannot
401 account for the full amplitude of sea ice variability and/or tend to have lower correlations during
402 periods of low variability (Figure 4 and 6). Qikiqtarjuaq, Rigby Island and Beechey Island
403 correlations to SIC were stronger after the 1980s, a period marked by higher variability of sea ice
404 and algal growth anomalies (Figure 6f, 6h, 6i). Similar to Qasigiannguit, correlations at
405 Qikiqtarjuaq of growth anomalies to SST have strengthened while those to SIC have decreased
406 (Figure 6f). In the Gulf of Boothia, correlations to SIC are strongest is the mid-record when SIC
407 and algal growth anomalies have high inter-annual variability (Figure 4g and 6g).
408
409 3.6 Inter-series variability
410
411 Synchrony of growth anomalies between samples from the same site was measured by first
412 conducting linear regression tests between algal anomaly time series sample pairs, and averaging
413 R-values together to express a site's inter-series correlation (R_{bar}), a statistic often used to express
414 synchrony in dendro- and sclerochronology (e.g., Butler et al., 2009). While inter-series
415 correlations at the annual level were only significant at one site, inter-series correlations were

416 significant at 5 sites when five-year running averages where used (Figure 7).
417

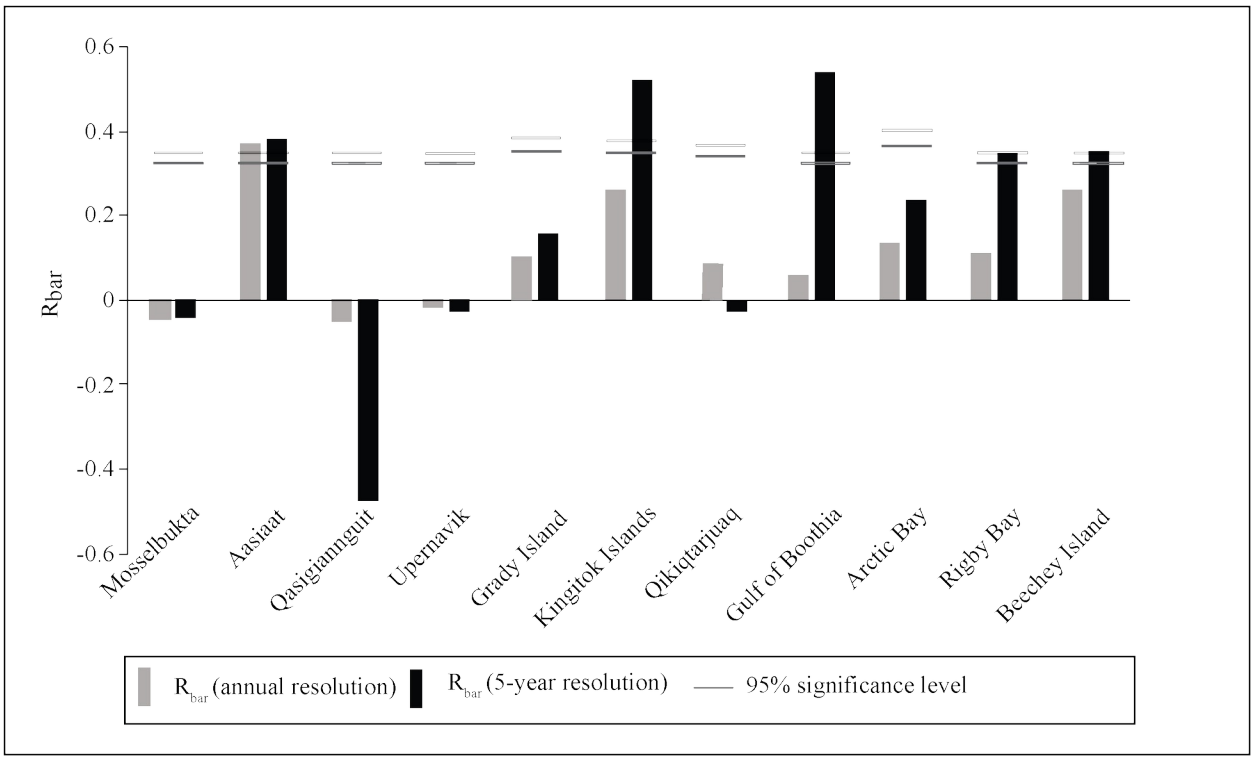

418

419 **Figure 7.** Inter-series correlation results (R_{bar}) at annual (grey) and five-year average (black)
420 resolutions with corresponding 95% significance level threshold (dark grey: annual resolution;
421 light grey: 5-year average resolution).

422 **4 Discussion**

423 4.1 Influence of runoff and degree of exposure on algal-ice relationships
424

425 Sites that significantly correlated with SIC_A and SIC_{SUMMER} tend to be in relatively exposed
426 regions, away from glacial and fluvial runoff sources. As was suggested by Adey et al. (2015)
427 these mid-exposure habitats in terms of currents and waves would likely yield the longest-lived
428 *C. compactum* specimens, as they would be affected by low levels of sedimentation and enough
429 grazers to remove sedimentary detritus on algal surfaces. Accordingly, growth may be more
430 affected by temperature or overlying sea ice if it is not impeded by grazers and/or sediment
431 accumulation. Sites that are relatively exposed include Beechey Island, Gulf of Boothia,
432 Qikiqtarjuaq, Kingitok Islands, and Upernavik as they are situated on islands away from the

433 coast or on peninsulas as opposed to embayments. Spatial correlation maps of these relatively
434 exposed sites showed strong negative correlations to SIC in grid cells radiating around collection
435 sites (Figure 5). This supports the hypothesis that *C. compactum* growth anomalies respond
436 firstly to local SIC conditions and, by association, secondarily to regional SIC conditions.
437 Slightly less exposed sites include Rigby Bay, Aasiaat and Qasigiannguit which are located near
438 the mouth of exposed bays. Algal growth increments are likely recording very localized light
439 variation when their locations are more secluded such as the Arctic Bay site in the Canadian
440 Arctic Archipelago. Arctic Bay's distance to more dynamic sea ice regions in the archipelago is
441 distinct from other sites investigated, leading to a low energy environment with possible
442 increased sediment buildup on the algae, thereby lowering receipt of light.
443
444 Furthermore, *C. compactum* samples are collected in nearshore environments, environments that
445 become increasingly vulnerable to higher sediment discharge with warming conditions and
446 reduced sea ice (Teichert & Freiwald, 2014). Accordingly, diminishing correlations between
447 algal growth anomalies and SST and/or SIC instrumental records may be enhanced in regions
448 near sediment runoff. Mosselbukta and Aasiaat experienced decreasing correlations with SIC
449 particularly noticeable in the 1990s into the early 2000s (Figure 6a & 6k) as SIC significantly
450 declined. While instrumental data for runoff is not available for Mosselbukta, Svalbard, modeled
451 runoff data suggested increasing runoff in recent decades (Lang, Fettweis, & Erpicum, 2015;
452 Möller & Kohler, 2018; Østby et al., 2017; van Pelt et al., 2016). Barium-calcium ratios (Ba/Ca)
453 in coralline red algae have previously been used to reconstruct variability in runoff in nearshore
454 environments (Chan et al., 2011). More recently, a study on *C. compactum* Ba/Ca from
455 Mosselbukta effectively suggested a drastic increase in runoff since the late 1980s (Hetzinger, et
456 al., 2021). This could have created more turbidity in the water column and less solar light
457 transmission to the benthos, causing a recent reduction in increment widths in the Mosselbukta
458 samples. The Aasiaat samples also exhibited a trend towards thinner growth increments in recent
459 years, while reduction of SIC should have caused an increase in growth, and could therefore also
460 be affected by increased sedimentation, especially due to the proximity to many glacial outputs
461 related to the Jakobshavn glacier near Illullisat, Greenland.
462
463 4.2 Ice-on duration effect on algal response to sea ice conditions

Williams et al. (2018) suggested that light plays a more significant role in *C. compactum*'s growth in warmer environments. While this may be true in ice-free regions with more balanced light and temperature controls, the results of this study showed that algal growth anomalies from regions with shorter ice-free seasons (i.e., shorter sunlight access) and lower sea surface temperatures (Table 2 and 3) were better able to record light-inhibition by ice cover than regions near the ice margin with longer ice-free seasons. This includes Beechey Island, Rigby Bay, Gulf of Boothia, Qikiqtarjuaq, Upernavik and Kingitok Islands in the Canadian Arctic Archipelago and on the central Labrador coast (Figure 2). Spatial correlation maps indicate that algal anomalies from these sites have strong relationships with regional SIC and ocean currents (Figure 5). Currents play a significant role in sea ice dynamics (Warn-Varnas, Allard, & Piacsek, 1991), causing similar sea ice conditions along them. Accordingly, these high correlation regions indicate which regions may yield future samples useful to reconstruct regional sea ice.

Upernavik, Grady Island and Kingitok Islands have all encountered a significant reduction in the length of the ice-free season. Upernavik has witnessed ice-free Julys since 1997, after which correlations with both sea ice and temperature were reduced (Figure 6c). After 1997, there were also marked reductions in algal growth increment variability and sea ice concentration (Figure 4c). This proceeded came after a positive Arctic Oscillation phase which decreased multi-year ice coverage and coincided with abnormally warm air temperatures after 1996 which expedited the rate of sea ice decline for the years to come (Overland & Wang, 2005). After the late 1990s, algal growth anomalies became less variable reflected also by low and stable sea ice concentrations. However, algal growth anomalies did not always match regional sea ice variability suggesting that other factors may have affected algal growth variability. Sea surface temperatures (SST) continued to increase and algal growth anomalies seemed to have responded to SST peaks but failed to increase in amplitude (Supplementary Figure 1). According to a recent study by He et al. (2019), cloud increased in the Upernavik region since the early 2000s. Previous work on the coralline red algae species *Lithothamnion glaciale*, found an inverse relationship between summer calcification and the previous winter's cloud cover in Scotland (Burdett, Kamenos, & Law, 2011). Therefore, while sea ice concentrations have reduced around Upernavik and produced a trend towards thicker growth increments, increased cloud cover may

have counteracted the effect of the longer ice-free season by dimming sunlight access to the sea floor, thereby reducing the inter-annual variability (i.e., amplitude) of growth increments (Figure 4c), and the correlation between sea ice and algal growth (Figure 6c) in the last decade of the record.

Similarly, in the early satellite record, ice-free conditions started in July and ended in November in the Kingitok Islands. However, after the early 2000s, the region was ice-free by June lasting until December in some years causing longer ice-free periods. The reduction of sea ice may have disrupted the previously stronger sea ice relationship with algal growth. Results of 10-year running correlations show that SIC_{SUMMER} and SST_{SUMMER} correlations with algal growth anomalies declined in the 2000s likely as a result of the lengthening of the ice-free period (Figure 6e). In the late record, algal anomalies no longer matched SIC variability but continued to match the trend towards less sea ice (larger increments) (Figure 4e). The region experienced relatively stable summer sea surface temperatures (1979-2010, June-July), while summer cloud cover reduced (-2.65% per decade, 1982-2010). Accordingly, the reduction of cloud cover would have increased the sunlight irradiance reaching algal specimens and may have produced larger increments in lower SIC years and increased the inter-annual variability of sunlight-driven growth.

On the other hand, while algal growth anomalies from Grady Island weakly correlated with the trend of instrumental records (Tables 2 and 3), they produced negative 10-year running correlations with SIC_{SUMMER} and SST_{SUMMER} (Figure 6a), suggesting they responded to sea ice variability. Since linear regressions are sensitive to trends, the fact that algal growth anomalies showed a strong trend towards smaller increments in the 2000s while deteriorating sea ice conditions typically bolster the formation of larger increments suggested that factors other than SST and SIC limited algal growth in recent time. Regional phytoplankton productivity time series (Glen Harrison et al., 2013) and chlorophyll α concentration from MODIS/Aqua satellite records suggested that the amplitude of algal anomalies may have been affected by summer phytoplankton productivity-caused turbidity. Years with higher summer Chlorophyll α concentrations often occur simultaneously with lower algal growth anomalies. Barium-calcium ratio and carbon isotopes time series derived from *C. compactum* have previously established the

526 relationship between coralline red algae geochemistry (Ba/Ca and $\delta^{13}C$) and sea ice driven
527 productivity variability (Chan et al., 2017). Due to the relationship between algal growth and
528 light availability, it is likely that turbidity caused by large phytoplankton blooms may have
529 affected the amplitude of algal growth anomalies especially in regions with longer ice-free
530 seasons.
531
532 In addition, algal growth anomalies from regions that experienced significant reductions in sea
533 ice cover may shift from being sea ice dependent to being temperature dependent, as exhibited
534 by the Qasigiannguit and Qikiqtarjuaq samples, while previously higher concentrations and
535 longer duration of sea ice may produce stronger algal-sea ice relationships. Previous studies
536 examined the multi-centennial Mosselbukta algal time series and revealed a strong relationship
537 between combined algal anomalies and sea ice cover from the early 20th century to the early
538 2000s (Hetzinger et al., 2019), demonstrating that the algal sea ice proxy had a higher recording
539 strength during periods and in regions of longer sea ice cover duration. Therefore, sea ice may
540 have variable control on algal growth anomalies depending on the length of the open water
541 season, when the annual solar insolation cycle, temperature and other light inhibiting variables
542 exert a stronger influence on algal growth, especially for sites closer to the margins of the ice
543 pack. In some regions, longer open water durations have produced large phytoplankton blooms
544 and increased cloud cover which could further obscure light reaching the seafloor and influence
545 *C. compactum* growth and geochemistry (Arrigo, van Dijken, & Pabi, 2008; Chan et al., 2017;
546 He et al., 2019). On the other hand, shorter ice-free periods may limit the effect light inhibitors
547 (excluding sea ice) have on annual algal growth anomalies.
548
549 4.3 Spatial resolution bias of the satellite record
550
551 Typically, the ice-free season is defined as less than 15% sea ice concentration (Ridley, et al.,
552 2016), providing a warmer open water period when photosynthetic growth of *C. compactum*
553 should be occurring (Adey, 1970; Williams et al., 2018). However, the data from this study
554 suggested that *C. compactum* grew and recorded SIC during months with higher than 15% sea
555 ice cover over the 75 km^2 gridded area (Figure 4). For example, regions such as Lancaster Sound
556 near Beechey Island had the strongest negative correlation of all sites (Table 2, Figure 5), but has

557 seldom recorded monthly means lower than 30% SIC over the study period. A 1° spatial
558 resolution SIC time series provided by the KNMI Climate Explorer tool revealed that months
559 with the strongest negative correlations at Beechey Island occurred during low SIC months (i.e.,
560 May-Oct) but SIC levels were rarely below 15% (Reynolds, et al., 2002). Further, NASA
561 satellite images showed ice breakup around Beechey Island by late July that was cleared of ice
562 by early August (2002-2015) suggesting that the lack of correlation between ice-free day/year
563 and algal growth anomalies (Table 2) may be caused by an inaccurate representation of local ice-
564 free and ice-on days in the 75 km^2 gridded satellite cell. Further, some issues regarding early
565 sensors and data homogenization (National Center for Atmospheric Research Staff, 2019) may
566 have challenged the comparison of satellite-derived SIC to algal anomalies as early satellite
567 imagery was unable to capture SIC in small channels and bays due to the presence of land within
568 large 25 km^2 grid cells (Howell, Duguay, & Markus, 2009). This is particularly noticeable in the
569 region around Arctic Bay, where satellite imagery showed some discrepancies in timing of ice
570 formation and breakup between the secluded setting of Arctic Bay and the adjacent larger inlet
571 which offered the nearest gridded SIC data (Supplemental Figure 2).
572
573 4.4 Temporal resolution of algal-ice relationship
574
575 The measure of ice-free days consists of very high-resolution temporal data; however, algae
576 likely start growing well before the database records <15% sea ice concentrations. Similarly,
577 photosynthetic phytoplankton start blooming while the ice is thin, uncovered by snow and full of
578 melt ponds (Massicotte et al., 2020) while daily satellite records would still record ice cover
579 (<15%). This may explain why few correlations were found between annual growth anomalies
580 and ice-free days. In addition, correlations with SIC were appreciably stronger when both growth
581 increment and SIC measurements were downsampled to 5-year running means (Table 2). *C.*
582 *compactum*'s growth increments have previously been shown to correlate well to long-term
583 regional sea ice decline over at least the past century (Halfar et al., 2013; Hetzinger et al., 2019).
584 Therefore, while able to record SIC on an annual scale, *C. compactum*'s may be better suited to
585 reconstruct SIC variability on a multi-year average scale (Hetzinger et al., 2019). The reasons for
586 this likely are that other light inhibitors such as sedimentation, phytoplankton blooms and cloud
587 cover may have affected the amplitude of algal anomalies for any given year. Therefore, 5-year

588 running averages may smooth out the impact of these other light-related variables. Furthermore,
589 five-year running means of algal growth time series produced significant inter-series correlations
590 at 5 sites, in comparison to 1 at an annual resolution (Figure 7). This suggested that either multi-
591 year averages reduced individual noise and isolated the climate signal or that multiyear averages
592 smoothed potential age model errors that may have reduced inter-series correlations at the annual
593 level.
594
595 4.5 Inter-sample variability
596
597 Uncertainties remain about how the number of algal samples included in site averages affects the
598 strength of the sea ice-algal proxy relationship. In this study all analyzed samples were included
599 in calculating algal growth anomalies, however the results clearly convey the variability between
600 samples and that poor inter-series correlations may have affected the final algal correlation with
601 sea ice conditions (Figure 6). Williams et al. (2014) suggested that inter-sample variability might
602 be caused by variation in micro-environments (e.g., sample positioning relative to shading on the
603 seafloor). On the other hand, Marali and Schöne (2015), who studied growth increments from the
604 North Atlantic bivalve *Arctica islandica*, suggested that periods of low inter-annual variability
605 could cause proxy time series from different samples to become desynchronized by factors
606 affecting the organism at the individual level. Accordingly, Aasiaat and Qasigiannguit algal
607 samples experienced reduced inter-annual summer SST variability (Jun-Jul) in recent record
608 years. Simultaneously, higher inter-sample growth variability was observed (Figure 4). During
609 low inter-annual climate variability, individual algal samples may be affected by differential
610 predation pressures from chitons and urchins, physical disturbances, and competitive overgrowth
611 may cause growth anomalies and consequent growth variability between samples (Adey et al.,
612 2013). It is important to note that some samples produced synchronous algal growth anomalies,
613 while the averaged inter-series correlation for the entire site was reduced significantly if a less
614 synchronous sample was integrated in the average. Therefore, it will be important to focus on
615 synchronous samples with a shared environmental signal when using *C. compactum* as a past sea
616 ice proxy.
617

In this study two to three samples per site were averaged, with the exception of Mosselbukta where five samples were averaged. In other proxy studies, the number of samples used is dependent on the proxy archive. Sediment core-based studies often rely on a single well-dated core sample (e.g., (Berben, et al., 2017; Eiríksson et al., 2011). Coral-based proxy time series are also typically generated from a single core sample from each site (e.g., Calvo et al., 2007; Tierney et al., 2015) due to the high cost of geochemical analysis and time involved to prepare and process data (Corrège, 2006). However, multi-sample proxy studies are becoming more common to increase replication, proxy signal strength and reliability (DeLong, et al., 2013; Jones et al., 2009; von Reumont, et al., 2016). Hetzinger et al. (2018) showed high replicability of Mg/Ca ratios down-sampled to 12 measurements/year from nine *C. compactum* sample collected in the Gulf of Maine, an ice-free region with larger growth increments, indicating their common climate signal. This theoretically suggests that only one algal sample could be used to build a time series. Conversely, colder and light-limited regions of the Arctic are more likely to produce thinner increments with unclear boundaries during high sea ice cover years which could introduce errors in age model construction. The results of 10-year running correlations at sites with long sea ice duration and high sea ice concentrations (i.e., Rigby Bay, Beechey Island, Gulf of Boothia) showed a reduction in correlation with instrumental SIC and SST records further back in time, suggesting possible errors propagated later into the record due to the thinner increments more easily missed when growth rates are slower in high SIC and colder periods. Further incorporation of cross-dating methods in age model construction may help diagnose synchrony problems and identify samples that should be excluded from *C. compactum*-based proxy reconstructions.

5 Conclusions

This is the first multi-sample study investigating the relationship between algal anomalies of *Clathromorphum compactum* (Mg/Ca, growth increment, and combined anomalies) and sea ice cover at multiple sites in the Arctic and Subarctic obtained from high spatial resolution satellite datasets. The results of this study showed that correlations between algal growth anomalies and sea ice concentration are stronger in regions/periods of higher sea ice concentrations, longer ice-on seasons, and reduced runoff and turbidity. Accordingly, our results yield important information for the identification of ideal study sites for future sea ice reconstructions. Annual

algal growth anomalies may be sufficient, instead of combined algal anomalies or Mg/Ca ratios alone, to show relative change in sea ice conditions at sites where algal anomalies respond more predictably to year-to-year sea ice variability. However, the algal growth proxy recorded SIC more strongly at most sites when downsampled to a five-year running mean and may therefore produce better reconstructions on a multi-year average scale. Spatial correlation maps showed that algal growth anomalies generally inversely correlated to regional SIC variability at most sites. Weaker correlations between growth increment anomalies and sea ice conditions may be related to differential exposure, turbidity, and lengthening of the ice-free season in the past two decades, while correlations with sea ice cover in earlier, higher sea ice cover periods prior to 1979 were likely stronger (e.g., Hetzinger et al., 2019). Furthermore, algal growth anomalies from regions that experienced significant reductions in sea ice cover may shift from being sea ice dependent to being temperature dependent. Questions remain regarding variability between samples and their timeseries as some sites tended to have low inter-series correlations. Synchronous growth within sites should be a requirement to reconstruct annually-resolved sea ice conditions of the past. The significant correlations between algal growth anomalies and SIC highlight the opportunity *C. compactum* can provide as an *in situ* marine high-resolution ice cover proxy.

Acknowledgments

Funding sources: NSERC Discovery (1303409; J.H.); NSERC CGS-D (CGSD3- 518838 - 2018; N.L.). Kent Moore and Marc DeBenedetti for MATLAB assistance. Miriam Pfeiffer for statistical insights. Doritt Jacob for analytical work at Mainz University. Authors acknowledge no conflict of interest.

Data

The data on which this article is based contains original data in combination with previously published data which are available in Halfar et al. (2013) and Hetzinger et al. (2019). Original datasets will be published through the NOAA National Centers for Environmental Information Paleoclimatology Data Repository (https://www.ncei.noaa.gov/pub/data/paleo/) upon acceptance. Primary datasets for this research are also included in figures and supplementary information files.

References

Adey, W. (1965). The genus Clathromorphum (Corallinaceae) in the Gulf of Maine. *Hydrobiologia*, *26*(3–4), 539–573.

Adey, W. H. (1970). The effects of light and temperature on growth rates in boreal−subarctic crustose corallines. *Journal of Phycology*, *6*(3), 269–276.

Adey, W. H., Halfar, J., & Williams, B. (2013). *The Coralline Genus Clathromorphum Foslie emend. Adey: Biological, Physiological, and Ecological Factors Controlling Carbonate Production in an Arctic-Subarctic Climate Archive*. Washington DC: Smithsonian Institution Scholarly Press.

Adey, W., Halfar, J., Humphreys, A., Suskiewicz, T., Belanger, D., Gagnon, P., & Fox, M. (2015). Subarctic rhodolith beds promote longevity of crustose coralline algal buildups and their climate archiving potential. *Palaios*, *30*(4), 281–293.

Arrigo, K. R., van Dijken, G., & Pabi, S. (2008). Impact of a shrinking Arctic ice cover on marine primary production. *Geophysical Research Letters*, *35*(19). https://doi.org/10.1029/2008GL035028

694 Backman, J., Jakobsson, M., Løvlie, R., Polyak, L., & Febo, L. A. (2004). Is the central Arctic
695 Ocean a sediment starved basin? *Quaternary Science Reviews*, *23*(11–13), 1435–1454.
696 https://doi.org/10.1016/J.QUASCIREV.2003.12.005
697 Belt, S. T. (2019). What do IP25 and related biomarkers really reveal about sea ice change?
698 *Quaternary Science Reviews*, *204*, 216–219.
699 https://doi.org/10.1016/J.QUASCIREV.2018.11.025
700 Belt, S. T., Brown, T. A., Rodriguez, A. N., Sanz, P. C., Tonkin, A., & Ingle, R. (2012). A
701 reproducible method for the extraction, identification and quantification of the Arctic sea
702 ice proxy IP25 from marine sediments. *Analytical Methods*, *4*(3), 705.
703 https://doi.org/10.1039/c2ay05728j
704 Belt, S. T., Massé, G., Rowland, S. J., Poulin, M., Michel, C., & LeBlanc, B. (2007). A novel
705 chemical fossil of palaeo sea ice: IP25. *Organic Geochemistry*, *38*(1), 16–27.
706 https://doi.org/10.1016/J.ORGGEOCHEM.2006.09.013
707 Berben, S. M. P., Husum, K., Navarro-Rodriguez, A., Belt, S. T., & Aagaard-Sørensen, S.
708 (2017). Semi-quantitative reconstruction of early to late Holocene spring and summer sea
709 ice conditions in the northern Barents Sea. *Journal of Quaternary Science*, *32*(5), 587–603.
710 https://doi.org/10.1002/jqs.2953
711 Burdett, H., Kamenos, N. A., & Law, A. (2011). Using coralline algae to understand historic
712 marine cloud cover. *Palaeogeography, Palaeoclimatology, Palaeoecology*, *302*(1), 65–70.
713 https://doi.org/10.1016/j.palaeo.2010.07.027
714 Butler, P. G., Scourse, J. D., Richardson, C. A., Wanamaker, A. D., Bryant, C. L., & Bennell, J.
715 D. (2009). Continuous marine radiocarbon reservoir calibration and the 13C Suess effect in
716 the Irish Sea: Results from the first multi-centennial shell-based marine master chronology.
717 *Earth and Planetary Science Letters*, *279*(3–4), 230–241.
718 https://doi.org/10.1016/j.epsl.2008.12.043
719 Calvo, E., Marshall, J. F., Pelejero, C., McCulloch, M. T., Gagan, M. K., & Lough, J. M. (2007).
720 Interdecadal climate variability in the Coral Sea since 1708 A.D. *Palaeogeography,*
721 *Palaeoclimatology, Palaeoecology*, *248*(1–2), 190–201.
722 https://doi.org/10.1016/j.palaeo.2006.12.003
723 Cavalieri, D. J., & Parkinson, C. L. (2012). Arctic sea ice variability and trends, 1979-2010. *The*
724 *Cryosphere*, *6*(4), 881–889. https://doi.org/https://doi.org/10.5194/tc-6-881-2012, 2012.

725 Chan, P., Halfar, J., Adey, W., Hetzinger, S., Zack, T., Moore, G. W. K., et al. (2017).
726 Multicentennial record of Labrador Sea primary productivity and sea-ice variability
727 archived in coralline algal barium. *Nature Communications*, *8*(1), 1–10.
728 https://doi.org/10.1038/ncomms15543
729 Chan, Phoebe, Halfar, J., Williams, B., Hetzinger, S., Steneck, R., Zack, T., & Jacob, D. E.
730 (2011). Freshening of the Alaska Coastal Current recorded by coralline algal Ba/Ca ratios.
731 *Journal of Geophysical Research*, *116*(G1), G01032.
732 https://doi.org/10.1029/2010JG001548
733 Comiso, J. C., Meier, W. N., & Gersten, R. (2017). Variability and trends in the Arctic Sea ice
734 cover: Results from different techniques. *Journal of Geophysical Research: Oceans*, *122*(8),
735 6883–6900. https://doi.org/10.1002/2017JC012768
736 Corrège, T. (2006). Sea surface temperature and salinity reconstruction from coral geochemical
737 tracers. *Palaeogeography, Palaeoclimatology, Palaeoecology*, *232*(2–4), 408–428.
738 https://doi.org/10.1016/j.palaeo.2005.10.014
739 De Vernal, A., Gersonde, R., Goosse, H., Seidenkrantz, M. S., & Wolff, E. W. (2013). Sea ice in
740 the paleoclimate system: The challenge of reconstructing sea ice from proxies - an
741 introduction. *Quaternary Science Reviews*, *79*, 1–8.
742 https://doi.org/10.1016/j.quascirev.2013.08.009
743 DeLong, K. L., Quinn, T. M., Taylor, F. W., Shen, C. C., & Lin, K. (2013). Improving coral-base
744 paleoclimate reconstructions by replicating 350 years of coral Sr/Ca variations.
745 *Palaeogeography, Palaeoclimatology, Palaeoecology*, *373*, 6–24.
746 https://doi.org/10.1016/j.palaeo.2012.08.019
747 Ding, Q., Schweiger, A., L'Heureux, M., Battisti, D. S., Po-Chedley, S., Johnson, N. C., et al.
748 (2017). Influence of high-latitude atmospheric circulation changes on summertime Arctic
749 sea ice. *Nature Climate Change*, *7*(4), 289–295. https://doi.org/10.1038/nclimate3241
750 Eiríksson, J., Knudsen, K. L., Larsen, G., Olsen, J., Heinemeier, J., Bartels-Jónsdóttir, H. B., et
751 al. (2011). Coupling of palaeoceanographic shifts and changes in marine reservoir ages off
752 North Iceland through the last millennium. *Palaeogeography, Palaeoclimatology,*
753 *Palaeoecology*, *302*(1), 95–108. https://doi.org/10.1016/j.palaeo.2010.06.002
754 Foster, M. S. (2001). Rhodoliths: Between rocks and soft places. *Journal of Phycology*, *37*(5),
755 659–667. https://doi.org/10.1046/j.1529-8817.2001.00195.x

Gemery, L., Cronin, T. M., Briggs, W. M., Brouwers, E. M., Schornikov, E. I., Stepanova, A., et al. (2017). An Arctic and Subarctic ostracode database: biogeographic and paleoceanographic applications. *Hydrobiologia*, *786*(1), 59–95. https://doi.org/10.1007/s10750-015-2587-4

Glen Harrison, W., Yngve Børsheim, K., Li, W. K. W., Maillet, G. L., Pepin, P., Sakshaug, E., et al. (2013). Phytoplankton production and growth regulation in the Subarctic North Atlantic: A comparative study of the Labrador Sea-Labrador/Newfoundland shelves and Barents/Norwegian/Greenland seas and shelves. *Progress in Oceanography*, *114*, 26–45. https://doi.org/10.1016/j.pocean.2013.05.003

Halfar, J., Adey, W. H., Kronz, A., Hetzinger, S., Edinger, E., & Fitzhugh, W. W. (2013). Arctic sea-ice decline archived by multicentury annual-resolution record from crustose coralline algal proxy. *Proceedings of the National Academy of Sciences* , *110*(49), 19737–19741. https://doi.org/10.1073/pnas.1313775110

He, M., Hu, Y., Chen, N., Wang, D., Huang, J., & Stamnes, K. (2019). High cloud coverage over melted areas dominates the impact of clouds on the albedo feedback in the Arctic. *Scientific Reports*, *9*(1), 1–11. https://doi.org/10.1038/s41598-019-44155-w

Hetzinger, S., Halfar, J., Kronz, A., Simon, K., Adey, W. H., & Steneck, R. S. (2018). Reproducibility of Clathromorphum compactum coralline algal Mg/Ca ratios and comparison to high-resolution sea surface temperature data. *Geochimica et Cosmochimica Acta*, *220*, 96–109.

Hetzinger, S., Halfar, J., Zack, T., Gamboa, G., Jacob, D. E., Kunz, B. E., et al. (2011). High-resolution analysis of trace elements in crustose coralline algae from the North Atlantic and North Pacific by laser ablation ICP-MS. *Palaeogeography, Palaeoclimatology, Palaeoecology*, *302*(1), 81–94. https://doi.org/10.1016/j.palaeo.2010.06.004

Hetzinger, Steffen, Halfar, J., Zajacz, Z., Möller, M., & Wisshak, M. (2021). Late twentieth century increase in northern Spitsbergen (Svalbard) glacier-derived runoff tracked by coralline algal Ba/Ca ratios. *Climate Dynamics*, *1*, 3. https://doi.org/10.1007/s00382-021-05642-x

Hetzinger, Steffen, Halfar, J., Zajacz, Z., & Wisshak, M. (2019). Early start of 20th-century Arctic sea-ice decline recorded in Svalbard coralline algae. *Geology*, *47*(10), 963–967. https://doi.org/10.1130/G46507.1

787 Hill, B. T., & Jones, S. J. (1990). The Newfoundland ice extent and the solar cycle from 1860 to
788 1988. *Journal of Geophysical Research*, *95*(C4), 5385.
789 https://doi.org/10.1029/JC095iC04p05385
790 Howell, S. EL, Duguay, C. R., & Markus, T. (2009). Sea ice conditions and melt season duration
791 variability within the Canadian Arctic Archipelago: 1979–2008. *Geophysical Research*
792 *Letters*, *36*(10). https://doi.org/10.1029/2009GL037681
793 Jones, P. D., Briffa, K. R., Osborn, T. J., Lough, J. M., Van Ommen, T. D., Vinther, B. M., et al.
794 (2009). High-resolution palaeoclimatology of the last millennium: A review of current
795 status and future prospects. *Holocene*, *19*(1), 3–49.
796 https://doi.org/10.1177/0959683608098952
797 Kaufman, D. S. (2009). An overview of late Holocene climate and environmental change
798 inferred from Arctic lake sediment. *Journal of Paleolimnology*, *41*(1), 1–6.
799 https://doi.org/10.1007/s10933-008-9259-6
800 Kinnard, C., Zdanowicz, C. M., Fisher, D. A., Isaksson, E., de Vernal, A., & Thompson, L. G.
801 (2011). Reconstructed changes in Arctic sea ice over thepast 1,450 years. *Nature*, *479*, 509–
802 513.
803 Köseoğlu, D., Belt, S. T., Husum, K., & Knies, J. (2018). An assessment of biomarker-based
804 multivariate classification methods versus the PIP25 index for paleo Arctic sea ice
805 reconstruction. *Organic Geochemistry*, *125*, 82–94.
806 https://doi.org/10.1016/j.orggeochem.2018.08.014
807 Kucera, M., Weinelt, M., Kiefer, T., Pflaumann, U., Hayes, A., Weinelt, M., et al. (2005).
808 Reconstruction of sea-surface temperatures from assemblages of planktonic foraminifera:
809 multi-technique approach based on geographically constrained calibration data sets and its
810 application to glacial Atlantic and Pacific Oceans. *Quaternary Science Reviews*, *24*, 951–
811 998. https://doi.org/10.1016/j.quascirev.2004.07.014
812 Lang, C., Fettweis, X., & Erpicum, M. (2015). Stable climate and surface mass balance in
813 Svalbard over 1979-2013 despite the Arctic warming. *Cryosphere*, *9*(1), 83–101.
814 https://doi.org/10.5194/tc-9-83-2015
815 Mahoney, A. R., Bockstoce, J. R., Botkin, D. B., Eicken, H., & Nisbet, R. A. (2011). Sea-Ice
816 distribution in the Bering and Chukchi seas: Information from historical whaleships'
817 logbooks and journals. *Arctic*, *64*(4), 465–477. Retrieved from

http://www.jstor.org/stable/41319241

Marali, S., & Schöne, B. R. (2015). Oceanographic control on shell growth of Arctica islandica (Bivalvia) in surface waters of Northeast Iceland — Implications for paleoclimate reconstructions. *Palaeogeography, Palaeoclimatology, Palaeoecology*, *420*, 138–149. https://doi.org/10.1016/j.palaeo.2014.12.016

Massicotte, P., Amiraux, R., Amyot, M. P., Archambault, P., Ardyna, M., Arnaud, L., et al. (2020). Green edge ice camp campaigns: Understanding the processes controlling the under-ice arctic phytoplankton spring bloom. *Earth System Science Data*, *12*(1), 151–176. https://doi.org/10.5194/essd-12-151-2020

Meier, W. N., Fetterer, F., Savoie, M., Mallory, S., Duerr, R., & Stroeve, J. (2017). *NOAA/NSIDC Climate Data Record of Passive Microwave Sea Ice Concentration*. Boulder, Colorado: NSIDC: National Snow and Ice Data Center. https://doi.org/https://doi.org/10.7265/N59P2ZTG

Meier, Walter N., Hovelsrud, G. K., Van Oort, B. E. H., Key, J. R., Kovacs, K. M., Michel, C., et al. (2014). Arctic sea ice in transformation: A review of recent observed changes and impacts on biology and human activity. *Reviews of Geophysics*, *52*(3), 185–217. https://doi.org/10.1002/2013RG000431

Melling, H. (2002). Sea ice of the northern Canadian Arctic Archipelago. *Journal of Geophysical Research: Oceans*, *107*(11), 2–1. https://doi.org/10.1029/2001jc001102

Möller, M., & Kohler, J. (2018). Differing climatic mass balance evolution across Svalbard glacier regions over 1900–2010. *Frontiers in Earth Science*, *6*, 128. https://doi.org/10.3389/feart.2018.00128

Müller, J., Wagner, A., Fahl, K., Stein, R., Prange, M., & Lohmann, G. (2011). Towards quantitative sea ice reconstructions in the northern North Atlantic: A combined biomarker and numerical modelling approach. *Earth and Planetary Science Letters*, *306*(3–4), 137–148. https://doi.org/10.1016/J.EPSL.2011.04.011

National Center for Atmospheric Research Staff. (2019). The Climate Data Guide: Sea Ice Concentration data from NOAA OI. Retrieved February 10, 2019, from Climate Data Guide website: https://climatedataguide.ucar.edu/climate-data/sea-ice-concentration-data-noaa-oi

Østby, T. I., Vikhamar Schuler, T., Ove Hagen, J., Hock, R., Kohler, J., & Reijmer, C. H. (2017). Diagnosing the decline in climatic mass balance of glaciers in Svalbard over 1957-2014.

Cryosphere, *11*(1), 191–215. https://doi.org/10.5194/tc-11-191-2017

Overland, J. E., & Wang, M. (2005). The Arctic climate paradox: The recent decrease of the Arctic Oscillation. *Geophysical Research Letters*, *32*(6), L06701. https://doi.org/10.1029/2004GL021752

Peng, G., Meier, W. N., Scott, D. J., & Savoie, M. H. (2013). A long-term and reproducible passive microwave sea ice concentration data record for climate studies and monitoring. *Earth System Science Data*, *5*(2), 311–318. https://doi.org/10.5194/essd-5-311-2013

Polyak, L., Alley, R. B., Andrews, J. T., Brigham-Grette, J., Cronin, T. M., Darby, D. A., et al. (2010). History of sea ice in the Arctic. *Quaternary Science Reviews*, *29*(15–16), 1757–1778. https://doi.org/10.1016/j.quascirev.2010.02.010

Ran, L., Jiang, H., Knudsen, K. L., & Eiríksson, J. (2011). Diatom-based reconstruction of palaeoceanographic changes on the North Icelandic shelf during the last millennium. *Palaeogeography, Palaeoclimatology, Palaeoecology*, *302*(1), 109–119. https://doi.org/10.1016/j.palaeo.2010.02.001

Rayner, N. A., Parker, D. E., Horton, E. B., Folland, C. K., Alexander, L. V., Rowell, D. P., et al. (2003). Global analyses of sea surface temperature, sea ice, and night marine air temperature since the late nineteenth century. *Journal of Geophysical Research*, *108*(D14), 4407. https://doi.org/10.1029/2002JD002670

Reynolds, R. W., Rayner, N. A., Smith, T. M., Stokes, D. C., & Wang, W. (2002). An improved in situ and satellite SST analysis for climate. *Journal of Climate*, *15*(13), 1609–1625. https://doi.org/10.1175/1520-0442(2002)015<1609:AIISAS>2.0.CO;2

Ridley, J. K., Wood, R. A., Keen, A. B., Blockley, E., & Lowe, J. A. (2016). Brief Communication: Does it matter exactly when the Arctic will become ice-free? *The Cryosphere Discussions*, 1–4. https://doi.org/10.5194/tc-2016-28

Seidenkrantz, M.-S. (2013). Benthic foraminifera as palaeo sea-ice indicators in the subarctic realm – examples from the Labrador Sea–Baffin Bay region. *Quaternary Science Reviews*, *79*, 135–144. https://doi.org/10.1016/J.QUASCIREV.2013.03.014

Sicre, M. A., Jacob, J., Ezat, U., Rousse, S., Kissel, C., Yiou, P., et al. (2008). Decadal variability of sea surface temperatures off North Iceland over the last 2000 years. *Earth and Planetary Science Letters*, *268*(1–2), 137–142. https://doi.org/10.1016/j.epsl.2008.01.011

Sicre, M. A., Yiou, P., Eiríksson, J., Ezat, U., Guimbaut, E., Dahhaoui, I., et al. (2008). A 4500-

year reconstruction of sea surface temperature variability at decadal time-scales off North Iceland. *Quaternary Science Reviews*, *27*(21–22), 2041–2047. https://doi.org/10.1016/j.quascirev.2008.08.009

Stein, R., & Fahl, K. (2013). Biomarker proxy shows potential for studying the entire Quaternary Arctic sea ice history. *Organic Geochemistry*, *55*, 98–102. https://doi.org/10.1016/J.ORGGEOCHEM.2012.11.005

Teichert, S., & Freiwald, A. (2014). Polar coralline algal CaCO3-production rates correspond to intensity and duration of the solar radiation. *Biogeosciences*, *11*(3), 833–842. https://doi.org/10.5194/bg-11-833-2014

Tierney, J. E., Abram, N. J., Anchukaitis, K. J., Evans, M. N., Giry, C., Kilbourne, K. H., et al. (2015). Tropical sea surface temperatures for the past four centuries reconstructed from coral archives. *Paleoceanography*, *30*(3), 226–252. https://doi.org/10.1002/2014PA002717

van Pelt, W. J. J., Kohler, J., Liston, G. E., Hagen, J. O., Luks, B., Reijmer, C. H., & Pohjola, V. A. (2016). Multidecadal climate and seasonal snow conditions in Svalbard. *Journal of Geophysical Research: Earth Surface*, *121*(11), 2100–2117. https://doi.org/10.1002/2016JF003999

von Reumont, J., Hetzinger, S., Garbe-Schönberg, D., Manfrino, C., & Dullo, W.-C. (2016). Impact of warming events on reef-scale temperature variability as captured in two Little Cayman coral Sr/Ca records. *Geochemistry, Geophysics, Geosystems*, *17*(3), 846–857. https://doi.org/10.1002/2015GC006194

Walsh, J. E., Fetterer, F., Stewart, S. J., & Chapman, W. L. (2017). A database for depicting Arctic sea ice variations back to 1850. *Geographical Review*, *107*(1), 89–107. https://doi.org/10.1111/j.1931-0846.2016.12195.x

Warn-Varnas, A., Allard, R., & Piacsek, S. (1991). Synoptic and seasonal variations of the ice-ocean circulation in the Arctic: a numerical study. *Annals of Glaciology*, *15*, 54–62. https://doi.org/10.1017/s026030550000954x

Williams, B., Halfar, J., DeLong, K. L., Hetzinger, S., Steneck, R. S., & Jacob, D. E. (2014). Multi-specimen and multi-site calibration of Aleutian coralline algal Mg/Ca to sea surface temperature. *Geochimica et Cosmochimica Acta*, *139*, 190–204. https://doi.org/10.1016/j.gca.2014.04.006

Williams, S., Adey, W. H., Halfar, J., Kronz, A., Gagnon, P., Bélanger, D., & Nash, M. (2018).

911 Effects of light and temperature on Mg uptake, growth, and calcification in the proxy
912 climate archive Clathromorphum compactum. *Biogeosciences*, *15*(19), 5745–5759.
913 Worley, S. J., Woodruff, S. D., Reynolds, R. W., Lubker, S. J., & Lott, N. (2005). ICOADS
914 Release 2.1 Data and Products. *Internaltional Journal of Climatology*, *25*, 823–842. https://
915 doi.org/10.1002/joc.1166
916